Inorganic Chemistry

Article

pubs.acs.org/IC

Oxidation of Glutathione by Hexachloroiridate(IV), Dicyanobis(bipyridine)iron(III), and Tetracyano(bipyridine)iron(III)

Nootan Bhattarai and David M. Stanbury*

Department of Chemistry and Biochemistry, Auburn University, Auburn, Alabama 36849, United States

Supporting Information

ABSTRACT: The aqueous oxidations of glutathione (GSH) by $[IrCl_6]^{2-}$, $[Fe(bpy)_2(CN)_2]^{+}$, and $[Fe(bpy)(CN)_4]^{-}$ are described. All three reactions are highly susceptible to catalysis by traces of copper ions, but this catalysis can be fully suppressed with suitable chelating agents. The direct oxidation by $[IrCl_6]^{2-}$ yields $[IrCl_6]^{3-}$ and GSO_3^{-}; some GSSG is also obtained in the presence of O_2. The two Fe^{III} oxidants are reduced to their corresponding Fe^{II} complexes with nearly quantitative formation of GSSG. The kinetics of these reactions have been studied at 25 °C and μ = 0.1 M between pH 1 and 11. All three reactions have rate laws that are first order in $[M_{ox}]$ and $[GSH]_t$ and show a general increase in rate with increasing pH. Detailed studies of the pH dependence enable the rate law to be elaborated with terms for reaction of the individual protonation states of GSH. These pH-resolved rate constants are interpreted with a mechanism having rate-limiting outer-sphere electron-transfer from the various thiolate forms of GSH.

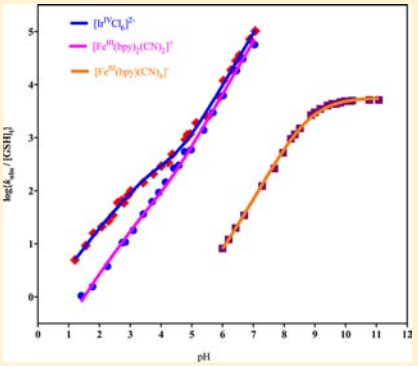

INTRODUCTION

Glutathione (GSH) (the tripeptide glutamyl-cysteinyl-glycine, Scheme 1) is the principal soluble thiol in plants and animals,

Scheme 1

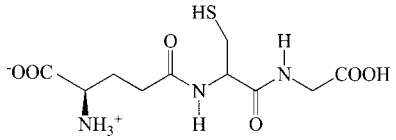

and it has extensive roles in cellular functions.[1,2] Prominent among these is its redox reactivity, including its important roles as a redox buffer and radical scavenger. When GSH functions as a radical scavenger it usually undergoes one-electron oxidation, which typically occurs initially at the cysteinyl sulfur group and yields the $GS^{\bullet}$ thiyl radical. Reports on the kinetics of aqueous oxidation of GSH by one-electron reagents include ferricytochrome c,[3] ferric salts,[4] Cu^{2+},[5] $[Co^{III}W_{12}O_{40}]^{5-}$,[6] $[Cu(TAAB)]^{2+}$,[7] Cr(VI),[8] $[Fe(bpy)_3]^{3+}$ and $[Fe(phen)_3]^{3+}$,[9] $[(Ru(bpy)_2(OH_2))_2O]^{4+}$,[10] $[Ru(edta)pz]^{-}$,[11] $[Fe(CN)_6]^{3-}$,[12] $[Fe^{IV}(O)(N4Py)]^{2+}$,[13] $[Mn^{III}(cdta)]^{-}$,[14] $[CrOO]^{2+}$,[15] $[Ru^{III}(NH_3)_5Cl]^{2+}$,[16] $[Ru^{III}(H_2O)_4Cl_2]^{+}$,[17] $[PV^{V}W_{11}O_{40}]^{4-}$ and $[PV^{V}_2W_{10}O_{40}]^{5-}$,[18] $ClO_2^{\bullet}$,[19] $NO_2^{\bullet}$,[20] $N_3^{\bullet}$,[21,22] $CO_3^{\bullet-}$,[23,24] $Br_2^{\bullet-}$,[25] $O_2^{\bullet-}$,[26] $OH^{\bullet}$,[27] $CH_3^{\bullet}$,[28] several alcohol radicals,[29] and the tyrosine phenoxyl radical.[30] These reports indicate a great diversity of rate laws and mechanisms, from which it is difficult to assemble a systematic understanding.

In principle, outer-sphere electron transfer could be an important pathway in GSH oxidations. An understanding of this pathway would contribute to building a systematic overview of GSH oxidations, since such reactions are well understood at the theoretical level, and there is a predictive framework (Marcus theory) for describing their rates. Studies of this type have already been published for two relatively simple thiols: the diprotic thioglycolic acid,[31−33] and the triprotic cysteine amino acid.[34,35] GSH, a tetraprotic acid, is the subject of the current study, which presents detailed investigations of the oxidation of GSH by three well-established outer-sphere reagents: $[IrCl_6]^{2-}$, $[Fe(bpy)_2(CN)_2]^{+}$, and $[Fe(bpy)(CN)_4]^{-}$. It shows that these reactions are highly sensitive to copper-ion catalysis, that the catalysis can be thoroughly inhibited with suitable chelating agents, that the uncatalyzed reactions have a common rate law, that the rate-limiting steps correspond to oxidation of the thiolate forms of GSH to the $GS^{\bullet}$ radical, and that the rates are consistent with Marcus theory. These results call into question some prior reports on GSH oxidation where copper-ion catalysis was not taken into consideration. They support other studies where electron transfer from the thiolate forms of GSH has been identified, and they complement reports of other oxidation mechanisms such as inner-sphere oxidation and hydrogen-atom transfer.

EXPERIMENTAL SECTION

Reagents and Solutions. NH_4Cl, acetic acid, monochloroacetic acid, $CuSO_4{\cdot}5H_2O$, $(NH_4)_2Fe(SO_4)_2{\cdot}6H_2O$, HNO_3, H_2SO_4, and chloroform (all from Fisher), cacodylic acid ($(CH_3)_2AsO_2H$), D_2O, GSH sulfonic acid (GSO_3H), and glycylglycine hydrochloride (gly gly) (all from Sigma), and *N*-*tert*-butyl-α-phenylnitrone (PBN, 98%), 2-6-pyridine dicarboxylic acid (dipic), 2,2′-bipyridyl (bpy), L-GSH (GSH, > 99%), L-GSH disulfide (GSSG), 3-(trimethylsilyl)-1-propane sulfonic acid sodium salt (DSS), tetraphenylphosphonium chloride (PPh_4Cl), and

Received: September 6, 2012
Published: November 27, 2012

   dx.doi.org/10.1021/ic301955y | *Inorg. Chem.* 2012, 51, 13303−13311

$(NH_4)_3IrCl_6·H_2O$ (all from Aldrich) were used without further purification. $NaCF_3SO_3$ (98%, GFS), EDTA (MCB), $K_3[Fe(CN)_6]$ (certified, Fisher), Cl_2 gas (Matheson), NaOH pellets ("SigmaUltra", Sigma-Aldrich), HCl, $NaHCO_3$ (J.T. Baker), ethanol, and Dowex 50-X8 resin (J.T. Baker) were used without further purification. $LiClO_4$ (GFS), and $NaClO_4$ (Fisher) were recrystallized from hot water. Anhydrous Na_3PO_4 was prepared from $Na_3PO_4·12H_2O$ (99.6% Fisher) by melting it in a muffle furnace at 150 °C followed by cooling, pulverization, and repeated heating at 150 °C for several hours.

$(NH_4)_2IrCl_6$ (Aldrich) was recrystallized by adding a saturated solution of NH_4Cl to a hot saturated solution of $(NH_4)_2IrCl_6$ (100 mg/14 mL H_2O). After cooling the mixture in an ice bath, the crystals were collected by vacuum filtration and washed with 20% $NH_4Cl_{(aq)}$ solution. Crystals were again washed with 95% ethanol two times (10 mL at a time) and finally with diethyl ether (10 mL portion two times). The crystals were air-dried first and then vacuum-dried.[36] Yield = 85%.

Deionized water was purified with a Barnstead Nanopure Infinity system and used to prepare all solutions. Freshly prepared solutions were used to run all experiments except for stock solutions of $NaClO_4$, $LiClO_4$, $HClO_4$, HCl, and some buffers. For all studies the reactant solutions were purged with argon gas on a bubbling line prior to use and transferred via glass syringes with Teflon or Pt needles, except where noted.

Stock solutions of $LiClO_4$ and $NaClO_4$ were standardized by titration. An aliquot was passed through a cation exchange column which had been packed with Dowex 50-X8 resin and regenerated with conc HCl. The eluate was then titrated with standard $NaOH_{(aq)}$ solution.

$[Fe(bpy)_2(CN)_2]·3H_2O$ was prepared and characterized as described in the literature.[37,38] Its ^1H NMR spectrum is in good agreement with prior reports.[39] **$[Fe(bpy)_2(CN)_2]NO_3$ and $K_2[Fe(bpy)(CN)_4]·3H_2O$** were made using Schilt's standard procedures.[34,37,38] The ^1H NMR spectrum of $K_2[Fe(bpy)(CN)_4]·3H_2O$ was in good agreement with a prior report.[39] **$Li[Fe(bpy)(CN)_4]·2.5H_2O$** was prepared with a slight modification of a published procedure:[34,40] A solution of $K_2[Fe(bpy)(CN)_4]$ was oxidized by sparging with an excess of Cl_2 gas. Then to the oxidized solution was added saturated hot solution of PPh_4Cl in 1:1 mol ratio. The solution turned to dirty yellow. The mixture was kept hot with constant stirring for about fifteen minutes, becoming a clear solution. The solution was cooled, and the resulting solid was collected by vacuum filtration. This $PPh_4[Fe^{III}(bpy)(CN)_4]$ was dissolved in acetonitrile, and then anhydrous $LiClO_4$ powder was added, keeping the ratio of 1:1.5 mols. A precipitate of $Li[Fe(bpy)(CN)_4]·2.5H_2O$ formed in high purity. Yield was 67%.

Methods. A HP-8453 diode array spectrophotometer equipped with a Brinkman Lauda RM6 thermostatted system was used to record all UV–vis spectra at 25 ± 0.1 °C; 10 mm quartz cells were used. All pH measurements were performed on a Corning 450 pH/ion meter with a Mettler Toledo Inlab 421 combination pH electrode, calibrated with standard buffers.

^1H NMR spectra were obtained on a Bruker AV 400 MHz spectrometer. Chemical shifts (δ, ppm) in D_2O were relative to DSS. In determining the product ratio for the anaerobic reaction of GSH with Ir^{IV}, noise was reduced by applying 0.3 Hz of line broadening (LB = 0.3); a value of LB = 2 was used for the experiment with exposure to O_2.

Electrochemical measurements were conducted on a BAS 100B electrochemical analyzer equipped with a BAS C3 cell stand provided with an N_2 purging and stirring system. The cell used a 3.2 mm diameter glassy carbon disk as a working electrode, a Ag/AgCl (3 M NaCl) reference electrode ($E°$ = 0.205 V vs NHE),[41] and a Pt wire auxiliary electrode.

Kinetic studies were done at 25 ± 0.1 °C on a Hi-Tech SF-51 stopped-flow spectrophotometer in the 1 cm path length configuration with Olis 4300 data acquisition and analysis software. The reactions of GSH with $(NH_4)_2IrCl_6$, $[Fe(bpy)_2(CN)_2]NO_3$, and $Li[Fe(bpy)(CN)_4]$ were monitored at 488, 522, and 482 nm respectively, always maintaining at least a 10-fold molar excess of GSH relative to the oxidant. All rate constants reported are the average of at least four runs unless and otherwise stated; shot-to-shot variation in k_{obs} was typically ±1–3%. Least-squares fits of the pseudo-first-order rate constants were performed with the Prism 5 software package,[42] weighting the data proportionally to the inverse square of k_{obs}. When fitting the pH-dependent rate laws, proton concentrations were calculated with the approximation $[H^+] = 10^{-pH}$.

Electrospray mass spectra were recorded with a Waters Q-Tof Premier mass spectrometer. Samples for positive-ion spectroscopy were acidified with 0.1% formic acid. Samples were injected via a 10 μL sample loop directly into the ESI source at a flow rate of 50 μL/min with 50% acetonitrile as the mobile phase.

RESULTS

Solution Properties of the Metal Complexes. The UV–vis spectra and $E_{1/2}$ (μ = 0.1 M) values for the three oxidants ($[IrCl_6]^{2-}$, $[Fe^{III}(bpy)_2(CN)_2]^+$, and $[Fe^{III}(bpy)(CN)_4]^-$) are summarized in Table 1. $(NH_4)_2IrCl_6$ has a characteristic UV–vis spectrum with a peak at 488 nm, in good agreement with prior reports.[43−45] The value for $\varepsilon_{488}(Ir^{IV})$ = 3980 M^{-1} cm^{-1} has an estimated uncertainty of ±4% based on the range in prior reports.[45−48] Its electrochemistry shows a reversible CV (cyclic voltammogram) corresponding to reduction to $[IrCl_6]^{3-}$ with $\Delta E_{p/p}$ = 64 mV and $E_{1/2}$ = 0.89 V vs NHE at μ = 0.1 M, also in good agreement with prior results.[49] $[Fe^{III}(bpy)_2(CN)_2]NO_3$ has a UV–vis spectrum as reported in the literature,[37] with the two peaks at wavelengths 394 and 544 nm (ε_{394} = 1382 and ε_{544} = 269 M^{-1} cm^{-1} respectively). Its CV is reversible with $\Delta E_{p/p}$ = 61 mV and $E_{1/2}$ = 0.77 V vs NHE, and this is in good agreement with the $E_{1/2}$ = 0.76 V obtained from OSWV. $Li[Fe^{III}(bpy)(CN)_4]$ displays a UV–vis spectrum that is quite stable at slightly acidic pH for two days. This absorbance spectrum has two characteristic peaks at 375 and 416 nm with ε_{375} = 1467 and ε_{482} = 975 M^{-1} cm^{-1}, in good agreement with the literature.[34] The CV of $Li[Fe^{III}(bpy)(CN)_4]$ is reversible ($\Delta E_{p/p}$ = 67 mV) with $E_{1/2}$ = 0. 55 V vs NHE, also in good agreement with prior reports.[34]

$[Fe^{II}(bpy)_2(CN)_2]$ has limited aqueous solubility (ca. 1 mM), which is a significant constraint on studies where it is involved. Its UV–vis spectrum displays two absorbance peaks at 352 and 522 nm with molar absorptivities of 5556 and 5848 M^{-1} cm^{-1} respectively, in good agreement with prior reports.[37] Its CV is essentially identical with that of $[Fe^{III}(bpy)_2(CN)_2]NO_3$. $K_2[Fe^{II}(bpy)(CN)_4]$ has a UV–vis spectrum with two characteristic peaks at 346 and 482 nm with ε_{346} = 3200 and ε_{482} = 2624 M^{-1} cm^{-1}, as has been reported previously.[34] Its CV is virtually identical with that of $Li[Fe^{III}(bpy)(CN)_4]$.

Table 1. Properties of the Coordination Complexes in Aqueous Solution

compound	band	λ_{max}, nm	ε, M^{-1} cm^{-1}	$E_{1/2}$, mV[a]
$(NH_4)_2[IrCl_6]$		488	3.98×10^3	704
$Fe^{II}(bpy)_2(CN)_2$	I	352	5.56×10^3	566
	II	522	5.85×10^3	
$[Fe^{III}(bpy)_2(CN)_2]NO_3$	I	394	1.38×10^3	566
	II	544	2.69×10^2	
$K_2[Fe^{II}(bpy)(CN)_4]$	I	346	3.20×10^3	351
	II	482	2.62×10^3	
$Li[Fe^{III}(bpy)(CN)_4]$	I	375	1.48×10^3	350
	II	416	9.63×10^2	

[a] μ = 0.1 M, mV vs Ag/AgCl.

Qualitative Features of the GSH Reactions. Rapid color changes ensue upon mixing solutions of GSH with the three oxidants. Reduction of $[IrCl_6]^{2-}$ is signaled by the loss of absorbance at 488 nm, while the reductions of $[Fe^{III}(bpy)_2(CN)_2]^+$

and $[Fe^{III}(bpy)(CN)_4]^-$ occur with absorbance increases at 522 and 482 nm, respectively.

As is typical of thiol oxidations by inert one-electron oxidants,[31−35] these three reactions are highly susceptible to catalysis by copper ions. For example, the addition of 1 μM $CuSO_4$ led to a 4-fold rate increase in the oxidation of GSH by $[IrCl_6]^{2-}$ at pH 4.6, a 3-fold rate increase in the oxidation by $[Fe^{III}(bpy)_2(CN)_2]^+$ at pH 4.7, and a 12-fold rate increase in the oxidation by $[Fe^{III}(bpy)(CN)_4]^-$ at pH 7.0 (Supporting Information, Tables S1−S3). On the other hand, the addition of 1 mM 2,6-dipicolinic acid (dipic), a well-established inhibitor of copper catalysis,[31,32,34,35] led to a 3-fold reduction in the rate of the $[IrCl_6]^{2-}$ reaction. Likewise, 2 mM dipic or 5 mM EDTA reduced the rate of the $[Fe^{III}(bpy)(CN)_4]^-$ reaction by a factor of 10. Moreover, in the presence of 1 mM dipic the $[IrCl_6]^{2-}$ reaction rate was unaffected by the addition of 5 μM $CuSO_4$, and in the presence of 5 mM EDTA the $[Fe^{III}(bpy)(CN)_4]^-$ reaction was unaffected by 5 μM $CuSO_4$. These results show that trace levels of Cu^{2+} ions as impurities are sufficient to dominate the reaction kinetics and that copper catalysis can be completely suppressed by the addition of suitable chelating agents. All results described below were obtained in the presence of these inhibitors. In the reaction of $[IrCl_6]^{2-}$ at pH 4.6, variation of the dipic concentration from 1 to 8 mM had no effect on the rates (Supporting Information, Table S4); accordingly, 1 mM dipic was deemed adequate; EDTA is unsuitable for use with $[IrCl_6]^{2-}$ because it is oxidized directly. EDTA can be used with $[Fe^{III}(bpy)(CN)_4]^-$ because this is a significantly weaker oxidant.

Stoichiometry with $[IrCl_6]^{2-}$. Using excess GSH over $[IrCl_6]^{2-}$, the Ir-containing product was identified and determined from UV−vis spectroscopy and electrochemistry (OSWV). For the UV−vis study, an unbuffered solution of 0.10 mM Ir^{IV} with 1 mM dipic and 0.1 M $NaClO_4$ was prepared, and its spectrum was recorded. Then, sufficient solid GSH was added to the Ir^{IV} solution to make a 1 mM GSH solution, and after reaction the spectrum was recorded. The spectra show complete consumption of Ir^{IV} and a product spectrum that is consistent with conversion to $[IrCl_6]^{3-}$ (Supporting Information, Figure S1). Upon chlorination of this product solution the original $[IrCl_6]^{2-}$ spectrum was recovered in full yield, confirming that reduction of $[IrCl_6]^{2-}$ by GSH proceeds without loss of bound chloride (Supporting Information, Figure S2). This inference is based on the well-established evidence that chlorination of aquated derivatives of $[IrCl_6]^{3-}$ yields the corresponding Ir^{IV} products, which have distinct UV−vis spectra.[45] Further evidence that the coordination sphere of $[IrCl_6]^{2-}$ remains intact during reduction by GSH is provided by OSWV (Osteryoung square wave voltammetry) (Supporting Information, Figure S3): here, a product solution was prepared from the reaction 0.1 mM Ir^{IV} and 1 mM GSH in 0.1 M $HClO_4$ and in the presence of 1 mM dipic. The solution was then chlorinated to remove the interfering excess GSH and oxidize the Ir^{III} to Ir^{IV}. OSWV analysis of this solution yielded a voltammogram having a peak potential and current closely consistent with an authentic sample of $[IrCl_6]^{2-}$. The aquo derivatives of $[IrCl_6]^{2-}$ have significantly higher $E°$ values.[50]

Sulfur-containing products were determined by electrospray mass spectrometry and ^{1}H NMR spectroscopy. Positive-ion mass analysis was performed on the products arising from the reaction of 1.0 mM GSH and 4.0 mM Ir^{IV} with 1 mM dipic at pH 3.2 where the reactants were exposed to O_2. Prominent peaks are evident at m/z 613.12 corresponding to GSSG and at m/z 356.068 corresponding to GSO_3H (Supporting Information, Figure S4). ^{1}H NMR analysis was performed on a solution of 1 mM GSH, 4.9 mM Ir^{IV}, and 1 mM dipic with a little DSS in D_2O that was allowed to react. The ^{1}H NMR spectrum of the product mixture (Supporting Information, Figure S5) shows complete consumption of the GSH and two different sets of peaks that are assigned to GSSG and GSH sulfonate (GSO_3^-). These two products have overlapping peaks in most regions of the spectrum, but they can be distinguished in the region between δ 3.2 and 3.5 ppm. In particular, GSO_3^- has an isolated doublet of doublets centered at 3.42 ppm corresponding to the cysteine C_β-H_b proton. The region between δ 3.23 and 3.32 ppm comprises a doublet of doublets due to the GSO_3^- cysteine C_β-H_a proton and an overlapping doublet of doublets arising from the pair of GSSG cysteine C_β-H_a protons.[51] An estimate of the product ratio, $[GSO_3^-]/[GSSG]$ = 6.4, can be calculated from the peak integrals as $2I_{3.42}/(I_{3.23-3.32} - I_{3.42})$. When a similar experiment was performed with solutions exposed to O_2 the $[GSO_3^-]/[GSSG]$ ratio was 2.1.

A spectrophotometric titration was conducted at pH 4.8 (acetate buffer) with 1 mM dipic. 2.0 mL of 0.276 mM GSH was placed in a cuvette and titrated under Ar with a 4.7 mM solution of Ir^{IV} (Supporting Information, Figure S6). These spectra show a weak absorbance increase at 420 nm associated with the formation of Ir^{III};[45] at the end point the spectra begin to show a much larger absorbance increase which is due to the accumulation of excess Ir^{IV}. The titration curve at 488 nm has a well-defined end point, corresponding to a molar consumption ratio $\Delta(Ir^{IV})/\Delta(GSH)$ of (7.1 ± 0.3) where the uncertainty reflects the precision of the end point and the uncertainty in the molar absorptivity of Ir^{IV}. When the titration was performed with exposure to O_2 the consumption ratio (= 4.2) was significantly smaller.

From these observations it is evident that the overall oxidation of GSH by $[IrCl_6]^{2-}$ under anaerobic conditions is given primarily by

$$6[IrCl_6]^{2-} + GSH + 3H_2O \rightarrow 6[IrCl_6]^{3-} + GSO_3^- + 7H^+ \quad (1)$$

A minor component of the reaction is disulfide formation:

$$2[IrCl_6]^{2-} + 2GSH \rightarrow 2[IrCl_6]^{3-} + GSSG + 2H^+ \quad (2)$$

The slight excess over 6 for the stoichiometric ratio obtained from the spectrophotometric titrations indicates a small degree of oxidation beyond the GSO_3^- stage, although the products were not identified.

Stoichiometry with $[Fe(bpy)_2(CN)_2]^+$. The ^{1}H NMR spectrum of the reaction products arising from an equimolar mixture of GSH and $[Fe^{III}(bpy)_2(CN)_2]^+$ shows that the Fe^{III} reagent is cleanly reduced to $[Fe^{II}(bpy)_2(CN)_2]$ (Supporting Information, Figure S7). This conclusion is based on the chemical shift values in the region 7.2−9.4 ppm, which are characteristic of $[Fe(bpy)_2(CN)_2]$.[39] The sharpness of these peaks is an indication that there is no residual Fe^{III} in the product mixture. The same NMR spectrum displays peaks due to GSSG at δ 3.291, 3.279, 3.255, and 3.244 ppm, and the lack of other peaks indicates that GSSG is the major oxidation product. UV−vis analysis of the reaction of 0.05 mM Fe^{III} with 0.5 mM GSH shows quantitative production (>95% yield) of $[Fe(bpy)_2(CN)_2]$ with its characteristic peak at 522 nm (Supporting Information, Figure S8). The consumption ratio $(\Delta[Fe(III)]/\Delta[GSH]_t$ = 1.5 ± 0.3) was obtained from a spectrophotometric titration of GSH with Fe^{III} at pH 4.7 (Supporting Information, Figure S9).

dx.doi.org/10.1021/ic301955y | Inorg. Chem. 2012, 51, 13303−13311

These results imply that the major overall reaction in excess GSH is

$$2[Fe^{III}(bpy)_2(CN)_2]^+ + 2GSH \rightarrow GSSG + 2[Fe^{II}(bpy)_2(CN)_2] + 2H^+ \quad (3)$$

A minor degree of overoxidation (oxidation beyond GSSG) is inferred from the excess consumption of Fe^{III}.

Stoichiometry with $[Fe^{III}(bpy)(CN)_4]^-$. Quantitative conversion (≥92%) of $[Fe^{III}(bpy)(CN)_4]^-$ to $[Fe^{II}(bpy)(CN)_4]^{2-}$ with excess GSH was observed by UV−vis spectroscopy (Supporting Information, Figure S10). This result was obtained when 0.05 mM Fe^{III} reacted with 2.0 mM GSH at pH 7.2 (gly gly buffer). The product spectrum has peaks at 346 and 482 nm characteristic of $[Fe^{II}(bpy)(CN)_4]^{2-}$, the yield of Fe^{II} being determined from the molar absorptivity at 482 nm. Conversion of $[Fe^{III}(bpy)(CN)_4]^-$ to $[Fe^{II}(bpy)(CN)_4]^{2-}$ is confirmed by the ^1H NMR product spectrum obtained under similar conditions, as shown in Supporting Information, Figure S11. This NMR spectrum also shows that GSSG is the only detected reaction product derived from GSH.

The consumption ratio in the reaction of $[Fe^{III}(bpy)(CN)_4]^-$ with GSH was determined at pH 6.3 by spectrophotometric titration of GSH, monitoring the absorbance at 482 nm (Supporting Information, Figure S12). At the end point, 2.0×10^{-6} moles of GSH consumed 2.41×10^{-6} moles of Fe^{III} indicating a stoichiometric ratio of 1.2 ± 0.2 (= Δ[Fe(III)]/$\Delta[GSH]_t$).

In view of the spectroscopic and titration results described above, the overall reaction is described by eq 4:

$$2[Fe^{III}(bpy)(CN)_4]^- + 2GSH \rightarrow GSSG + 2[Fe^{II}(bpy)(CN)_4]^{2-} + 2H^+ \quad (4)$$

Kinetics, General Features. As described above, copper ions are strongly catalytic in the reactions of all three oxidants with GSH. Accordingly, all kinetic results described below are obtained from reactions conducted in the presence of inhibitors that completely suppress the catalysis. The reactions were generally studied with a flooding excess of GSH over oxidant, which led to pseudo-first-order kinetics. The pseudo-first-order rate constant (k_{obs}) is defined by eq 5, where M_{ox} = Ir^{IV} and Fe^{III}:

$$-d[M_{ox}]/dt = k_{obs}[M_{ox}] \quad (5)$$

GSH has four acidic protons, with pK_{a1} = 2.12, pK_{a2} = 3.512, pK_{a3} = 8.73, and pK_{a4} = 9.65 at ionic strength 0.1 M.[19,52] Thus, GSH potentially has five kinetically distinguishable protonation states: cationic (protonated), neutral, monoanionic, dianionic, and trianionic forms depending upon pH, which are represented as $HGSH^+$, GSH^0, GSH-H^-, GSH-$2H^{2-}$, and GSH-$3H^{3-}$, respectively. In principle, each of these protonation states could be reactive. The total GSH concentration is designated $[GSH]_t$. Under the assumption that these protonation states are rapidly interconverted and that each protonation state reacts with simple mixed second-order kinetics, the general rate law is eq 6:

$$k_{obs} = k[GSH]_t = k_1[HGSH^+] + k_2[GSH^0] + k_3[GSH\text{-}H^-] + k_4[GSH\text{-}2H^{2-}] + k_5[GSH\text{-}3H^{3-}] \quad (6)$$

Inclusion in eq 6 of all respective pK_a terms leads to eq 7:

$$k_{obs} = \left[\frac{k_1[H^+]^4 + k_2K_{a1}[H^+]^3 + k_3K_{a1}K_{a2}[H^+]^2 + k_4K_{a1}K_{a2}K_{a3}[H^+] + k_5K_{a1}K_{a2}K_{a3}K_{a4}}{[H^+]^4 + K_{a1}[H^+]^3 + K_{a1}K_{a2}[H^+]^2 + K_{a1}K_{a2}K_{a3}[H^+] + K_{a1}K_{a2}K_{a3}K_{a4}}\right][GSH]_t \quad (7)$$

At a given pH eq 7 simplifies to

$$k_{obs} = k_{pH}[GSH]_t \quad (8)$$

Deviations from rate law 5 can be anticipated for weak oxidants under acidic conditions, when inhibition by the product M_{red} can occur in thiol oxidations.[31,32,34,35] No such inhibition was detected in the current study with $[IrCl_6]^{2-}$ as the oxidant. As is described below, the reactions of the weaker oxidants $[Fe(bpy)_2(CN)_2]^+$ and $[Fe(bpy)(CN)_4]^-$ showed mild product inhibition kinetics. Following prior practice,[31,32,34,35] these effects were eliminated by use of the radical spin trap PBN.

Kinetics with $[IrCl_6]^{2-}$. A typical kinetic trace with an excellent pseudo-first-order fit is obtained for the reaction of Ir^{IV} with GSH under the conditions $[Ir^{IV}]$ = 0.1 mM, $[GSH]_t$ = 1.0 mM, pH = 4.6 (10 mM acetate buffer), [dipic] = 1.0 mM, and μ = 0.1 M ($NaClO_4$) (Supporting Information, Figure S13). In another experiment under these conditions the buffer concentration was reduced by a factor of 10 (1 mM buffer), and virtually identical results were obtained. This latter result implies that the rate law is independent of buffer concentration.

The dependence on $[GSH]_t$ was investigated at pH 4.5 ± 0.1 (acetate buffer) over a 10-fold range in GSH concentration, with 0.1 mM $[Ir^{IV}]_0$, 1.0 mM dipic, $[GSH]_t$ = 1.0−10 mM and 0.1 M ionic strength ($NaClO_4$) (Supporting Information, Table S5). The plot of k_{obs} vs $[GSH]_t$ shown in Figure 1 is linear, with a slope (7.42 ± 0.15) × 10^2 M^{-1} s^{-1} and intercept (0.14 ± 0.03) s^{-1}, and it confirms the rate law to be first order with respect to $[GSH]_t$ as in eq 8.

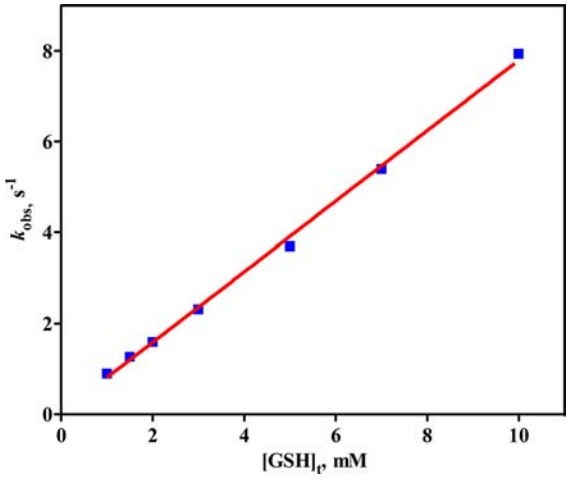

Figure 1. GSH dependence of k_{obs} in the reaction of $[IrCl_6]^{2-}$ with GSH. Solid line is a linear fit. $[Ir^{IV}]_0$ = 0.01 mM, $[GSH]_t$ = 1.0−10 mM, acetate buffer at pH 4.5 ± 0.1, with 1 mM dipic, μ = 0.1 M ($NaClO_4$). Standard deviations of the shot-to-shot k_{obs} values are smaller than the square data points.

dx.doi.org/10.1021/ic301955y | Inorg. Chem. 2012, 51, 13303−13311

The pH dependence was studied over the pH range 1.2−7.07, keeping the conditions 0.5−1.0 mM $[GSH]_t$, 1.0 mM dipic and 0.1 M ionic strength. Appropriate buffers were used to maintain pH between pH 2.4 and pH 7.1. Above pH 2.4 the ionic strength was maintained by $NaClO_4$, but, in order to minimize the effects of specific activity coefficients, below pH 2.4 the ionic strength was maintained with $LiClO_4$. All kinetic data are summarized in Supporting Information, Table S6. The plot of $\log(k_{obs}/[GSH]_t)$ vs pH shown in Figure 2 indicates a complex dependence on pH with an irregular trend of increasing rate with increasing pH, including a narrow plateau region around pH 4.5. Parenthetically, the slowest rates, obtained at low pH, were mildly sensitive to the purity of the $[IrCl_6]^{2-}$, presumably because of catalysis by aquated derivatives of this oxidant; similar catalysis has been reported for the oxidation of NH_2OH by $[IrCl_6]^{2-}$.[53] The data in Figure 2 were analyzed in accordance with eq 7, holding K_{a1}, K_{a2}, K_{a3} and K_{a4} at their literature values. Initial attempts to fit all five rate constants failed to converge, but an excellent fit to this equation was obtained by holding $k_5 = 0$. The pH-resolved second-order rate constants are $k_1 = 1.1 \pm 1.0\ M^{-1}\ s^{-1}$, $k_2 = 36 \pm 4\ M^{-1}\ s^{-1}$, $k_3 = (2.9 \pm 0.2) \times 10^2\ M^{-1}\ s^{-1}$, and $k_4 = (4.73 \pm 0.18) \times 10^6\ M^{-1}\ s^{-1}$ (rate constants collected in Table 2). Thus, k_1 is zero within its uncertainty, and k_5 is also undefined. In principle, k_5 could have been measured by conducting experiments at higher pH, but the rates become too fast to measure with our instrument under such conditions.

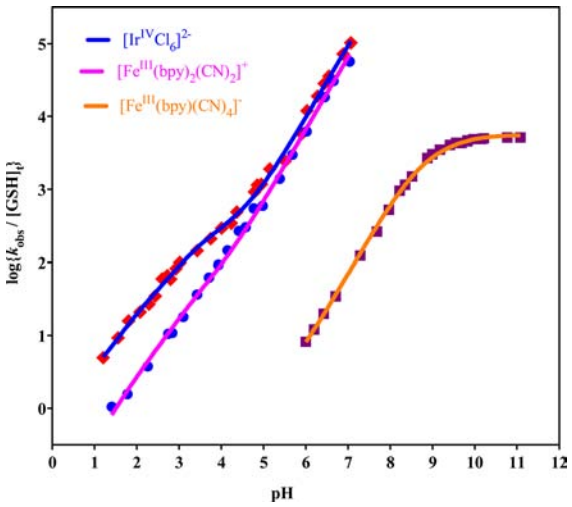

Figure 2. Plots of $\log(k_{obs}/[GSH]_t)$ vs pH for the reactions of GSH with $[IrCl_6]^{2-}$, $[Fe(bpy)_2(CN)_2]^+$, and $[Fe(bpy)(CN)_4]^-$. Red diamonds = experimental data for $[IrCl_6]^{2-}$, blue circles = exp. data for $[Fe(bpy)_2(CN)_2]^+$, purple squares = exp. data for $[Fe(bpy)(CN)_4]^-$. Solid lines are the fits to eq 7. Standard deviations of the shot-to-shot k_{obs} values are smaller than the square data points.

Table 2. pH-Resolved Rate Constants for the Oxidation of GSH[a]

parameter	$[IrCl_6]^{2-}$	$[Fe(bpy)_2(CN)_2]^+$	$[Fe(bpy)(CN)_4]^-$
k_1, $M^{-1}\ s^{-1}$	(1.1 ± 1.0)		
k_2, $M^{-1}\ s^{-1}$	36 ± 4	4.4 ± 0.5	
k_3, $M^{-1}\ s^{-1}$	$(2.9 \pm 0.2) \times 10^2$	59 ± 6	1.25 ± 0.5
k_4, $M^{-1}\ s^{-1}$	$(4.73 \pm 0.18) \times 10^6$	$(3.3 \pm 0.2) \times 10^6$	$(3.59 \pm 0.08) \times 10^3$
k_5, $M^{-1}\ s^{-1}$			$(5.5 \pm 0.2) \times 10^3$

[a] 25.0 °C, μ = 0.1 M.

The reaction of GSSG with $[IrCl_6]^{2-}$ was investigated in a separate experiment, since GSSG is one of the products of reaction of GSH with $[IrCl_6]^{2-}$ and its oxidation could conceivably lead to the formation of GSO_3^-. The experiment was performed at pH 5.0 (cacodylate buffer) with 0.17 mM $[IrCl_6]^{2-}$ and 0.15 mM GSSG. No appreciable loss of $[IrCl_6]^{2-}$ was detected over 1 h, which means that the second-order rate constant for reaction of GSSG with $[IrCl_6]^{2-}$ is less than 0.5 $M^{-1}\ s^{-1}$ at pH 5. This is considerably slower than the rate of reaction of $[IrCl_6]^{2-}$ with GSH at any pH.

Kinetics with $[Fe(bpy)_2(CN)_2]^+$. The kinetics of oxidation of GSH by $[Fe^{III}(bpy)_2(CN)_2]^+$ is mildly inhibited by $[Fe^{II}(bpy)_2(CN)_2]$ at lower pH. For example, the reaction of 0.5 mM GSH with 0.05 mM Fe^{III} at pH 6.0 occurred with k_{obs} = 4.3 s^{-1}, but k_{obs} decreased to 3.3 s^{-1} with 0.10 mM added Fe^{II}. At pH 6.7 the effect of Fe^{II} is weaker. At pH 3.2 the effect is strong enough to cause significant departures from pseudo-first-order kinetics (Supporting Information, Figure S14). The addition of 0.1 mM PBN is sufficient to prevent Fe^{II} inhibition, and it leads to excellent pseudo-first-order kinetics (Supporting Information, Figure S14). Accordingly, 0.1 mM PBN was included in all further kinetic measurements at pH 4.4 and below.

The dependence of k_{obs} on $[GSH]_t$ was determined at pH 4.3 (acetate buffer), maintaining the conditions $[Fe^{III}]$ = 0.05 mM, $[GSH]_t$ = 0.50−6.0 mM, [dipic] = 1.0 mM, [PBN] = 0.1 mM and μ = 0.1 M ($NaClO_4$) (Supporting Information, Table S7). These data demonstrate a linear dependence of k_{obs} on $[GSH]_t$ with a slope of 198 ± 4 $M^{-1}\ s^{-1}$ and a nearly insignificant intercept of 0.02 ± 0.005 s^{-1} (Supporting Information, Figure S15).

A study of the pH dependence of k_{obs} was performed over a broad range of pH (1.7−7.04) with $[Fe^{III}]_0$ = 0.05 mM, $[GSH]_t$ = 1.0 mM, [dipic] = 1.0 mM, and μ = 0.1 M (Li- or $NaClO_4$). The kinetic data are presented in Supporting Information, Table S8. The plot of this pH dependence in Figure 2 is rather similar to that for the oxidation by $[IrCl_6]^{2-}$, except that the rates are somewhat slower and the plateau around pH 4 is less evident. Fits of the data to rate law 7 failed to converge when holding K_{a1}, K_{a2}, K_{a3}, and K_{a4} at their literature values and allowing all five rate constants to be optimized. On the other hand, an excellent fit was obtained when the k_1 and k_5 terms were excluded from the rate law. The derived rate constants are $k_2 = 4.4 \pm 0.5\ M^{-1}\ s^{-1}$, $k_3 = 59 \pm 6\ M^{-1}\ s^{-1}$, and $k_4 = (3.3 \pm 0.2) \times 10^6\ M^{-1}\ s^{-1}$ (also collected in Table 2).

Kinetics with $[Fe^{III}(bpy)(CN)_4]^-$. The oxidation of GSH by $[Fe^{III}(bpy)(CN)_4]^-$ shows general similarities to the oxidations by $[IrCl_6]^{2-}$ and $[Fe^{III}(bpy)_2(CN)_2]^+$, except that it is generally slower. As a result, it was investigated at higher pH than the other two reactions. The reaction is also more sensitive to copper catalysis, showing significant departures from pseudo-first-order kinetics even with 2 mM dipic (Supporting Information, Table S3). Experiments on the reaction at pH 6.9 showed that phosphate buffer is ineffective at suppressing copper catalysis. It was found, however, that 5 mM EDTA is effective in suppressing copper catalysis and yields excellent pseudo-first-order kinetics. Because of the relatively high pH in the kinetics measurements, inhibition by Fe^{II} was quite mild (Supporting Information, Figure S16), and thus no PBN was added to the reactions.

The dependence of k_{obs} on $[GSH]_t$ was investigated at pH 7.28 (cacodylate buffer) with $[GSH]_t$ = 0.50−5.0 mM, $[Fe^{III}]_0$ = 0.05 mM, [EDTA] = 5.0 mM, and μ = 0.1 M ($NaClO_4$) (Supporting Information, Table S9). A linear dependence on

dx.doi.org/10.1021/ic301955y | Inorg. Chem. 2012, 51, 13303−13311

$[GSH]_t$ is obtained (Supporting Information, Figure S17) with a slope of 74.1 ± 1.8 M^{-1} s^{-1} and a negligible intercept of 0.004 ± 0.002 s^{-1}.

The pH dependence of k_{obs} was studied over the pH range 6.00−11.06, with the other conditions being $[Fe^{III}]_0$ = 0.05 mM, $[GSH]_t$ = 0.50−2.0 mM, [EDTA] = 5.0 mM, and μ = 0.1 M ($NaClO_4$). The kinetic data are summarized in Supporting Information, Table S10 and displayed in Figure 2. An excellent fit of the data with eq 7 was achieved by omitting the k_1 and k_2 terms, as shown in Figure 2. The derived second order rate constants are k_3 = 1.25 ± 0.5 M^{-1} s^{-1}, k_4 = (3.59 ± 0.08) × 10^3 M^{-1} s^{-1}, and k_5 = (5.5 ± 0.2) × 10^3 M^{-1} s^{-1} (also collected in Table 2). Although the k_3 value is only marginally significant, the k_4 and k_5 values are quite well resolved.

Kinetics with $[Fe^{III}(CN)_6]^{3-}$. The reaction of GSH with $[Fe(CN)_6]^{3-}$ was examined briefly, monitoring the consumption of $[Fe(CN)_6]^{3-}$ at 420 nm by conventional UV−vis spectrophotometry. When a reaction mixture was prepared containing 2.5 mM GSH and 0.10 mM $[Fe(CN)_6]^{3-}$ in 0.1 M phosphate buffer at pH 7.1, the reaction was rapid, with a half-life of less than 5 s. Under the same conditions except for the addition of 1 mM dipic the reaction was much slower, with a half-life of about 200 s. Because of the slowness of the reaction and the potential for catalysis by ligated metal ions,[54] further studies were not performed.

DISCUSSION

A notable trend in the oxidations of GSH by $[IrCl_6]^{2-}$, $[Fe^{III}(bpy)_2(CN)_2]^+$, and $[Fe(bpy)(CN)_4]^-$ is the increasing degree of overoxidation (formation of GSO_3^- rather than GSSG) with increasing $E°$ of the oxidant. An analogous trend is obtained in the oxidation of cysteine by $[Mo(CN)_8]^{3-}$, $[Fe^{III}(bpy)_2(CN)_2]^+$, and $[Fe(bpy)(CN)_4]^-$, although the overoxidation product is cysteine sulfinic acid rather than the sulfonate.[34,35] In the case of oxidation of thioglycolate by $[IrCl_6]^{2-}$ and $[Mo(CN)_8]^{3-}$ it is again only the stronger oxidant ($[IrCl_6]^{2-}$) that causes overoxidation, and in this case the product is the sulfonate.[32,33] Since $[IrCl_6]^{2-}$ reacts much more slowly (if at all) with GSSG than with GSH, it is clear that GSO_3^- must be produced from reaction intermediates before they generate GSSG.

A simplified general mechanism for reaction of GSH with the oxidants is given below. Details relating to the pH dependence of the rate-limiting steps are discussed further below.

$$M_{ox} + GSH \rightleftharpoons M_{red} + GS^{\bullet} + H^+ \quad (9)$$

$$GS^{\bullet} + GSH \rightleftharpoons GSSG^{\bullet -} + H^+ \quad (10)$$

$$M_{ox} + GSSG^{\bullet -} \rightarrow M_{red} + GSSG \quad (11)$$

$$2GS^{\bullet} \rightarrow GSSG \quad (12)$$

$$M_{ox} + GS^{\bullet} + H_2O \rightarrow M_{red} + GSOH + H^+ \quad (13)$$

$$GSOH + 2H_2O \rightarrow GSO_3^- + 4e^- + 5H^+ \quad (14)$$

$$GS^{\bullet} + PBN \rightarrow GSPBN^{\bullet} \quad (15)$$

Reaction 9 is the predominant rate-limiting step, which generates the well-known GSH thiyl radical. Reversibility in this reaction is indicated because of the observed kinetic inhibition by M_{red}. Production of H^+ in this step accounts in part for the enhanced inhibition by M_{red} in solutions that are more acidic. Reversible association of $GS^{\bullet}$ with GSH to form $GSSG^{\bullet -}$ in the next step (eq 10) is quite well established,[27,55,56] and its pH dependence also affects the kinetic inhibition by M_{red}. Two routes to GSSG are depicted in reactions 11 and 12. The first of these, oxidation of $GSSG^{\bullet -}$ by M_{ox}, is expected to have a large rate constant and to be predominant at higher pH. At lower pH, where reaction 10 is unfavorable, dimerization of $GS^{\bullet}$ could become significant. Formation of GSO_3^- is proposed to occur through the direct reaction of $GS^{\bullet}$ with M_{ox} as in eq 13; this reaction would lead initially to GSOH. Conversion of GSOH to GSO_3^- is indicated in eq 14, although the details of this conversion are unknown. Reaction 15 is the scavenging of $GS^{\bullet}$ by the spin trap PBN,[57] which is rapid enough to compete with the reverse of eq 9 and thus prevent kinetic inhibition by M_{red}.

By analogy with cysteine, it can be expected that GSOH reacts with GSH to form GSSG:[58]

$$GSOH + GSH \rightarrow GSSG + H_2O \quad (16)$$

The yield of GSO_3^- should thus be determined by the competition between reactions 16 and 14.

It is well-known that the GSH radical $GS^{\bullet}$ undergoes a reversible internal carbon-to-sulfur hydrogen-atom transfer reaction to yield $^{\bullet}GSH$.[59] It is possible that under acidic conditions where reaction 10 is disfavored and with weak oxidants where reaction 13 is insignificant, this internal hydrogen atom transfer could become competitive with $GS^{\bullet}$ dimerization. This could lead to more highly oxidized products. Although no such products were detected in the current study, the high stoichiometric ratio obtained for the Ir^{IV}/GSH reaction might be a consequence of this reaction pathway.

The effect of O_2 on the stoichiometry of the reaction of GSH with Ir^{IV} can be rationalized as a consequence of O_2 oxidizing the $GSSG^{-\bullet}$ radical:

$$GSSG^{-\bullet} + O_2 \rightarrow GSSG + O_2^{-\bullet} \quad (17)$$

This type of reaction is very rapid (k = 5.1 × 10^8 M^{-1} s^{-1})[60] because the $GSSG^{-\bullet}$ radical is strongly reducing.[61,62]

GSH has four acid/base sites: two carboxylates, a primary amine, and a thiol. In its cationic form, $HGSH^+$, all four sites are protonated. pK_{a1} and pK_{a2} lead to production of GSH^0 and $GSH\text{-}H^-$, which are primarily deprotonated at the carboxylate sites. pK_{a3} (= 8.73) corresponds to formation of $GSH\text{-}2H^{2-}$, which is mostly in the thiolate form. The primary amine site is the most strongly basic and is deprotonated at pK_{a4}.[63] The three intermediate protonation states can exist as various tautomers, and some of the microscopic equilibrium constants among them have been determined.[63] The pH dependence of the kinetics is accounted for by a model in which the various protonation states of GSH react with the oxidants:

$$GSH^0 + M_{ox} \rightarrow GS^{\bullet} + M_{red} \qquad k_2 \quad (18)$$

$$GSH\text{-}H^- + M_{ox} \rightarrow GS^{\bullet} + M_{red} \qquad k_3 \quad (19)$$

$$GSH\text{-}2H^{2-} + M_{ox} \rightarrow GS^{\bullet} + M_{red} \qquad k_4 \quad (20)$$

$$GSH\text{-}3H^{3-} + M_{ox} \rightarrow GS^{\bullet} + M_{red} \qquad k_5 \quad (21)$$

Despite considerable effort, we were unable to find evidence for reaction of $HGSH^+$ (k_1) with any of the three oxidants. This species is fully protonated and provides no possibility for tautomerization to expose a reactive thiolate form. On the other hand, the trianion $GSH\text{-}3H^{3-}$ is fully deprotonated, so it is unambiguously a thiolate. Reaction via this species is thus demonstrated by the well-resolved value of k_5 for $[Fe(bpy)(CN)_4]^-$.

dx.doi.org/10.1021/ic301955y | Inorg. Chem. 2012, 51, 13303−13311

It is inferred that the values of k_2, k_3, and k_4 in Table 2 all refer to reactions of the oxidants with the associated thiolate forms of GSH. Since the dianion GSH-2H^{2-} is primarily in the thiolate form, the values of k_4 are the actual bimolecular rate constants for the thiolate. On the other hand, for the species GSH^0 and GSH-H$^-$ the thiolate forms are the minor tautomers with the respective tautomerization equilibrium constants K_{Tn} and K_{Ta} being much less than unity:

$$HS{-}(NH_3^+)(COOH)(COO^-) \rightleftharpoons {}^-S{-}(NH_3^+)(COOH)_2 \qquad K_{Tn} \quad (22)$$

$$HS{-}(NH_3^+)(COO^-)_2^- \rightleftharpoons {}^-S{-}(NH_3^+)(COOH)(COO^-) \qquad K_{Ta} \quad (23)$$

$$^-S{-}(NH_3^+)(COOH)_2 + M_{ox} \rightarrow {}^\bullet S{-}(NH_3^+)(COOH)_2 + M_{red} \qquad k_{2a} \quad (24)$$

$$^-S{-}(NH_3^+)(COOH)(COO^-) + M_{ox} \rightarrow {}^\bullet S{-}(NH_3^+)(COOH)(COO^-) + M_{red} \qquad k_{3a} \quad (25)$$

These considerations lead to the relationships $k_2 = k_{2a}K_{Tn}$ and $k_3 = k_{3a}K_{Ta}$. A value of about 10^{-5} can be estimated for K_{Tn} and K_{Ta} from the known values for pK_{a2} and pK_{a3}. Values of the corrected bimolecular rate constants for the thiolate forms with the three oxidants are presented in Table 3. These data show that for a given oxidant the rate constants for the various thiolate forms lie within a range of a factor of 20, which is much smaller than the uncorrected range in Table 2. Evidently, protonation at the carboxylate and amine sites has relatively little influence on the corrected rate constants.

Table 3. Rate Constants for the Oxidation of the Thiolate Forms of GSH[a]

parameter	$[IrCl_6]^{2-}$	$[Fe(bpy)_2(CN)_2]^+$	$[Fe(bpy)(CN)_4]^-$
E_p, V vs NHE	0.89	0.77	0.55
k_{11}, M^{-1} s^{-1}	2×10^5[b]	6×10^5[c]	6×10^5[c]
k_{2a}, M^{-1} s^{-1}	4×10^6	4×10^5	
k_{3a}, M^{-1} s^{-1}	3×10^7	6×10^6	1×10^5
k_4, M^{-1} s^{-1}	4.7×10^6	3.3×10^6	3.6×10^3
k_5, M^{-1} s^{-1}			5.5×10^3

[a] 25.0 °C, μ = 0.1 M. Values for k_{2a} and k_{3a} derived from the values for k_2 and k_3 by adjusting for tautomerization. [b] Reference 70. [c] Reference 34.

An electron-transfer mechanism is assigned above to the reactions of the thiolate forms of GSH. This assignment is based on the observation that the metal complexes are reduced by one electron while retaining their coordination spheres intact. Further evidence for an electron-transfer mechanism is the kinetic inhibition by the reduced metal complex and the effects of the radical scavenger PBN. An estimate for the electron-transfer equilibrium constants can be made, making use of the E° values for the oxidants (shown in Table 3) and $E^\circ(GS^\bullet/GS^-)$ for the GSH thiyl radical. This latter quantity is estimated to be about 0.82 ± 0.02 V vs NHE.[64] Values for the derived electron-transfer equilibrium constants are 15 for $[IrCl_6]^{2-}$, 0.14 for $[Fe(bpy)_2(CN)_2]^+$, and 2×10^{-5} for $[Fe(bpy)(CN)_4]^-$. Values for the rate constants for reverse electron-transfer can be calculated from the forward rate constants in Table 3 and the equilibrium constants. In all cases except one they are well below the limits of diffusion control. The one exceptional case, $[Fe(bpy)(CN)_4]^-$, has a value of 5×10^9 M^{-1} s^{-1} for k_{-3a}, which is right at the diffusion limit for a reaction of this charge type. These calculations provide further evidence that these reactions have an electron-transfer mechanism.

As mentioned above, with $[IrCl_6]^{2-}$ as the oxidant, the thiolate electron-transfer equilibrium constants are about 15, that is, mildly favorable for products. The corresponding rate constants in Table 3 are several orders of magnitude smaller than the diffusion-controlled values, so a significant kinetic barrier can be inferred. If it is assumed that these electron-transfer reactions have an outer-sphere mechanism, then the cross relationship of Marcus theory should apply to the rate constants. Qualitatively, the rate constants in Table 3 decrease with decreasing E° for the oxidants, as expected from the Marcus cross relationship. When this relationship is applied in its usual form including work terms,[65] we calculate a self-exchange rate constant of 1×10^6 M^{-1} s^{-1} for the GSH-2H^{2-}/GS$^\bullet$ redox couple. This calculation is based on the value for k_4 in Table 3 for $[IrCl_6]^{2-}$, a self-exchange rate constant of 2×10^5 M^{-1} s^{-1} for $[IrCl_6]^{2-/3-}$, and radii of 4.1 Å for $[IrCl_6]^{2-}$ and 3 Å for GSH. Given the considerable uncertainties involved, this calculated self-exchange rate constant is quite similar to the value of 7×10^6 M^{-1} s^{-1} that was reported for the analogous cysteine self-exchange rate constant.[34]

These results are broadly consistent with those previously reported for oxidation of GSH by $ClO_2^\bullet$,[19] $NO_2^\bullet$,[20] $CO_3^{\bullet-}$,[23,24] and $N_3^\bullet$,[21,22] in that it is the thiolate forms of GSH that are reactive. Although the hydroxyl radical oxidizes GS$^-$ directly, it also oxidizes GSH, presumably through a hydrogen-atom abstraction mechanism.[66] This outcome is not unexpected, since OH$^\bullet$ is well-known as a H-atom abstractor.[67] With $CH_3^\bullet$, $Br_2^{\bullet-}$, alcohol radicals, and the tyrosinyl radical as oxidants it is unclear whether the reactions occur through GS$^-$ or GSH, since pH dependent measurements were not performed;[25,28−30,68] however, hydrogen-atom transfer from GSH to $CH_3^\bullet$ is likely, since an electron-transfer mechanism (producing CH_3^-) can be ruled out on the basis of its driving force ($E^\circ(CH_3^\bullet/CH_3^-)$ = −0.75 V).[69] A hydrogen-atom-transfer mechanism seems virtually assured for the alcohol radicals as well.[29] Ferric salts and $[Mn(cdta)]^-$ react through inner-sphere mechanisms.[4,14] Superoxide ($O_2^{\bullet-}$) is proposed to react through a chain reaction involving a highly unusual formal O$^+$ transfer from $O_2^{\bullet-}$ to GSH.[26] In the case of $[Fe(CN)_6]^{3-}$, a publication describes the results of a pH-dependent study in which a rate constant corresponding to k_3 of 300 M^{-1} s^{-1} was obtained;[12] regrettably, no precautions seem to have been taken to prevent copper-ion catalysis. In view of the rate constants in Table 2 and the low E° for $[Fe(CN)_6]^{3-}$, the value for k_3 seems to be too large by several orders of magnitude. Our brief observations on this reaction (described above) show that it is highly sensitive to metal-ion catalysis and that when dipic is added the rates are at least a factor of 500 slower than reported previously.[12] The reactions of $[Fe(bpy)_3]^{3+}$ and $[Fe(phen)_3]^{3+}$ might be expected to have the same rate laws as are reported here, but in fact are claimed to be first order in [H$^+$].[9] The reactions of $[PV^VW_{11}O_{40}]^{4-}$ and $[PV^V{}_2W_{10}O_{40}]^{5-}$ are reported to be second-order in [GSH].[18] We suggest that these latter anomalous results may also be due to unrecognized copper-ion catalysis.

In summary, when suitable precautions are taken to prevent copper-ion catalysis the oxidations of GSH by typical outer-sphere reagents follow the patterns already established for reactions of thioglycolic acid and cysteine. These patterns include (1) formation of GSSG with an increasing degree of overoxidation with stronger oxidants, (2) kinetic inhibition by the reduced

dx.doi.org/10.1021/ic301955y | Inorg. Chem. 2012, 51, 13303−13311

oxidants at low pH, (3) rate laws that are first order in [oxidant] and in $[GSH]_t$, (4) increasing rates with increasing pH, (5) undetectably low reactivity of the fully protonated species, (6) mechanisms in which only the thiolate forms undergo electron transfer, and (7) rate constants that increase with increasing E° of the oxidant.

■ ASSOCIATED CONTENT

Supporting Information

Tables of kinetic data, 9 pages. Figures of spectra, electrochemistry, and titrations, 12 pages. Figures of kinetic data, 5 pages. This material is available free of charge via the Internet at http://pubs.acs.org.

■ AUTHOR INFORMATION

Corresponding Author

*David M. Stanbury: email: stanbdm@auburn.edu.

Notes

The authors declare no competing financial interest.

■ ACKNOWLEDGMENTS

This research was supported by a grant from the NSF (# 0509889).

■ REFERENCES

(1) Sies, H. *Free Radical Biol. Med.* **1999**, *27*, 916−921.
(2) Meister, A.; Anderson, M. E. *Annu. Rev. Biochem.* **1983**, *52*, 711−760.
(3) Everse, J.; Kujundzic, N. *Biochemistry* **1979**, *18*, 2668−2673.
(4) Hamed, M. Y.; Silver, J.; Wilson, M. T. *Inorg. Chim. Acta* **1983**, *78*, 1−11.
(5) Scarpa, M.; Momo, F.; Viglino, P.; Vianello, F.; Rigo, A. *Biophys. Chem.* **1996**, *60*, 53−61.
(6) Ayoko, G. A.; Olatunji, M. A. *Inorg. Chim. Acta* **1983**, *80* (L15-L17), 287.
(7) Labuda, J.; Vanickova, M.; Pavlishchuk, V. V.; Kolchinskii, A. G. *Chem. Pap.* **1994**, *48*, 78−81.
(8) Bose, R. N.; Moghaddas, S.; Gelerinter, E. *Inorg. Chem.* **1992**, *31*, 1987−1994.
(9) Ayoko, G. A.; Iyun, J. F.; Ekubo, A. T. *Indian J. Chem.* **1993**, *32A*, 616−618.
(10) Ayoko, G. A.; Iyun, J. F.; Ekubo, A. T. *Transition Met. Chem.* **1993**, *18*, 6−8.
(11) Chatterjee, D.; Pal, U.; Ghosh, S.; van Eldik, R. *Dalton Trans* **2011**, *40*, 1302−1306.
(12) Stochel, G.; Martinez, P.; van Eldik, R. *J. Inorg. Biochem.* **1994**, *54*, 131−140.
(13) Campanali, A. A.; Kwiecien, T. D.; Hryhorczuk, L.; Kodanko, J. J. *Inorg. Chem.* **2010**, *49*, 4759−4761.
(14) Gangopadhyay, S.; Ali, M.; Dutta, A.; Banerjee, P. *J. Chem. Soc., Dalton Trans.* **1994**, 841−845.
(15) Perez-Benito, J. F.; Arias, C. *J. Phys. Chem. A* **1998**, *102*, 5837−5845.
(16) Frasca, D. R.; Clarke, M. J. *J. Am. Chem. Soc.* **1999**, *121*, 8523−8532.
(17) Nayak, S.; Brahma, G. S.; Reddy, K. V. *Aust. J. Chem.* **2012**, *65*, 113−120.
(18) Sami, P.; Anand, T. D.; Premanathan, M.; Rajasekaran, K. *Transition Met. Chem.* **2010**, *35*, 1019−1025.
(19) Ison, A.; Odeh, I. N.; Margerum, D. W. *Inorg. Chem.* **2006**, *45*, 8768−8775.
(20) Ford, E.; Hughes, M. N.; Wardman, P. *Free Radical Biol. Med.* **2002**, *32*, 1314−1323.
(21) Abedinzadeh, Z.; Gardes-Albert, M.; Ferradini, C. *Radiat. Phys. Chem.* **1991**, *38*, 1−5.
(22) Zhao, R.; Lind, J.; Merényi, G.; Eriksen, T. E. *J. Am. Chem. Soc.* **1994**, *116*, 12010−12015.
(23) Chen, S.-N.; Hoffman, M. Z. *Radiat. Res.* **1973**, *56*, 40−47.
(24) Eriksen, T. E.; Fransson, G. *Radiat. Phys. Chem.* **1988**, *32*, 163−167.
(25) Candeias, L. P.; Folkes, L. K.; Dennis, M. F.; Patel, K. B.; Everett, S. A.; Stratford, M. R. L.; Wardman, P. *J. Phys. Chem.* **1994**, *98*, 10131−10137.
(26) Winterbourn, C. C.; Metodiewa, D. *Free Radical Biol. Med.* **1999**, *27*, 322−328.
(27) Mezyk, S. P. *J. Phys. Chem.* **1996**, *100*, 8861−8866.
(28) Huston, P.; Espenson, J. H.; Bakac, A. *Inorg. Chem.* **1992**, *31*, 720−722.
(29) Schöneich, C.; Asmus, K. D.; Bonifacic, M. *J. Chem. Soc., Faraday Trans.* **1995**, *91*, 1923−1930.
(30) Folkes, L. K.; Trujillo, M.; Bartesaghi, S.; Radi, R.; Wardman, P. *Arch. Biochem. Biophys.* **2011**, *506*, 242−249.
(31) Hung, M.; Stanbury, D. M. *Inorg. Chem.* **2005**, *44*, 9952−9960.
(32) Saha, B.; Hung, M.; Stanbury, D. M. *Inorg. Chem.* **2002**, *41*, 5538−5543.
(33) Sun, J.; Stanbury, D. M. *J. Chem. Soc., Dalton Trans.* **2002**, 785−791.
(34) Wang, X.; Stanbury, D. M. *Inorg. Chem.* **2008**, *47*, 1224−1236.
(35) Hung, M.; Stanbury, D. M. *Inorg. Chem.* **2005**, *44*, 3541−3550.
(36) Kauffman, G. B.; Teter, L. A. *Inorg. Synth.* **1966**, *8*, 223−227.
(37) Schilt, A. A. *J. Am. Chem. Soc.* **1960**, *82*, 3000−3005.
(38) Wang, X.; Stanbury, D. M. *Inorg. Chem.* **2006**, *45*, 3415−3423.
(39) Agarwala, B. V.; Ramanathan, K. V.; Khetrapal, C. L. *J. Coord. Chem.* **1985**, *14*, 133−137.
(40) Lescouezec, R.; Lloret, F.; Julve, M.; Vaissermann, J.; Verdaguer, M. *Inorg. Chem.* **2002**, *41*, 818−826.
(41) Sawyer, D. T.; Sobkowiak, A.; Roberts, J. L. *Electrochemistry for Chemists*, 2nd ed; John Wiley and Sons: New York, 1995; pp 192.
(42) *Prism 5*; GraphPad Software, Inc.: San Diego, CA, 2010.
(43) Chang, J. C.; Garner, C. S. *Inorg. Chem.* **1965**, *4*, 209−215.
(44) Jorgensen, C. K. *Acta Chem. Scand.* **1957**, *11*, 151−165.
(45) Poulsen, I. A.; Garner, C. S. *J. Am. Chem. Soc.* **1962**, *84*, 2032−2037.
(46) Sarala, R.; Stanbury, D. M. *Inorg. Chem.* **1990**, *29*, 3456−3460.
(47) Stapp, E. L.; Carlyle, D. W. *Inorg. Chem.* **1974**, *13*, 834−837.
(48) Wilmarth, W. K.; Stanbury, D. M.; Byrd, J. E.; Po, H. N.; Chua, C.-P. *Coord. Chem. Rev.* **1983**, *51*, 155−179.
(49) Margerum, D. W.; Chellappa, K. L.; Bossu, F. P.; Burce, G. L. *J. Am. Chem. Soc.* **1975**, *97*, 6894−6896.
(50) Cecil, R.; Littler, J. S.; Easton, G. *J. Chem. Soc. B* **1970**, 626−631.
(51) Harwood, D. T.; Nimmo, S. L.; Kettle, A. J.; Winterbourn, C. C.; Ashby, M. T. *Chem. Res. Toxicol.* **2008**, *21*, 1011−1016.
(52) Krezel, A.; Bal, W. *Org. Biomol. Chem.* **2003**, *1*, 3885−3890.
(53) Makarycheva-Mikhailova, A. V.; Stanbury, D. M.; McKee, M. L. *J. Phys. Chem. B* **2007**, *111*, 6942−6948.
(54) Bridgart, G. J.; Wilson, I. R. *J. Chem. Soc., Dalton Trans.* **1973**, 1281−1284.
(55) Hoffman, M. Z.; Hayon, E. *J. Phys. Chem.* **1973**, *77*, 990−996.
(56) Mezyk, S. P.; Armstrong, D. A. *J. Chem. Soc., Perkin Trans. 2* **1999**, 1411−1419.
(57) Polovyanenko, D. N.; Plyusnin, V. F.; Reznikov, V. A.; Khramtsov, V. V.; Bagryanskaya, E. G. *J. Phys. Chem. B* **2008**, *112*, 4841−4847.
(58) Nagy, P.; Ashby, M. T. *J. Am. Chem. Soc.* **2007**, *129*, 14082−14091.
(59) Hofstetter, D.; Nauser, T.; Koppenol, W. H. *Chem. Res. Toxicol.* **2010**, *23*, 1596−1600.
(60) Prütz, W. A.; Butler, J.; Land, E. J. *Biophys. Chem.* **1994**, *49*, 101−111.
(61) Asmus, K.-D.; Bonifacic, M. In *S-Centered Radicals*; Alfassi, Z. B., Ed.; John Wiley & Sons: New York, 1999; pp 141−191.
(62) Quintiliani, M.; Badiello, R.; Tamba, M.; Esfandi, A.; Gorin, G. *Int. J. Radiat. Biol.* **1977**, *32*, 195−202.
(63) Rabenstein, D. L. *J. Am. Chem. Soc.* **1973**, *95*, 2797−2803.

(64) Madej, E.; Wardman, P. *Arch. Biochem. Biophys.* **2007**, *462*, 94−102.
(65) Zuckerman, J. J. *Inorganic Reactions and Methods*; VCH: Deerfield Beach, FL, 1986; Vol. *15*, pp 13−47.
(66) Mezyk, S. P. *Radiat. Res.* **1996**, *145*, 102−106.
(67) Stanbury, D. M. In *Physical Inorganic Chemistry: Reactions, Processes, and Applications*; Bakac, A., Ed.; John Wiley and Sons: Hoboken, NJ, 2010; pp 395−428.
(68) Cudina, I.; Jovanovic, S. V. *Radiat. Phys. Chem.* **1988**, *32*, 497−501.
(69) Warren, J. J.; Tronic, T. A.; Mayer, J. M. *Chem. Rev.* **2010**, *110*, 6961−7001.
(70) Hurwitz, P.; Kustin, K. *Trans. Faraday Soc.* **1966**, *62*, 427−432.